Articles

Bisphosphonate Inhibitors of *Toxoplasma gondi* Growth: In Vitro, QSAR, and In Vivo Investigations

Yan Ling,[‡] Gurmukh Sahota,[||] Sarah Odeh,[§] Julian M. W. Chan,[§] Fausto G. Araujo,[†] Silvia N. J. Moreno,[‡,⊥,*] and Eric Oldfield[||,§,*]

Laboratory of Molecular Parasitology, Department of Pathobiology and Center for Zoonoses Research, University of Illinois at Urbana-Champaign, 2001 South Lincoln Avenue, Urbana, Illinois, 61802; Department of Biophysics, University of Illinois at Urbana-Champaign, 600 South Mathews Avenue, Urbana, Illinois 61801; Department of Chemistry, University of Illinois at Urbana-Champaign, 600 South Mathews Avenue, Urbana, Illinois, 61801; and Department of Infectious Diseases, Palo Alto Medical Foundation, Palo Alto, California, 94301

Received July 9, 2004

We have investigated the activity of 60 bisphosphonates against the replication of *Toxoplasma gondii* in vitro and of three of the most active compounds, in vivo. The two most active compounds found were *n*-alkyl bisphosphonates containing long ($n = 9$ or 10) hydrocarbon chains, not the nitrogen-containing species used in bone resorption therapy. The target of all of the most active bisphosphonates appears to be the isoprene biosynthesis pathway enzyme farnesyl pyrophosphate synthase (FPPS), as indicated by the correlations between *T. gondii* growth inhibition and FPPS (human and *Leishmania major*) enzyme inhibition and by the fact that a *T. gondii* strain engineered to overexpress FPPS required considerably higher levels of bisphosphonates to achieve 50% growth inhibition, while the IC_{50} for atovaquone (which does not inhibit FPPS) remained the same in the overexpressing strain. The phosphonate inhibitor of the non-mevalonate pathway, fosmidomycin, which inhibits the enzyme 1-deoxy-xylulose-5-phosphate reductoisomerase, had no effect on *T. gondii* growth. To investigate structure−activity relationships (SARs) in more detail, we used two three-dimensional quantitative SAR methods: comparative molecular field analysis (CoMFA) and comparative molecular similarity indices analysis (CoMSIA), to investigate all 60 bisphosphonates. Both the CoMFA and CoMSIA models indicated a 60−70% contribution from steric interactions and a 30−40% contribution from electrostatic interactions and using four $N = 55$ training sets for each method, we found on average between a factor of 2 and 3 error in IC_{50} prediction. The three most active compounds found in vitro were tested in vivo in a Smith-Webster mouse model and the two most active bisphosphonates were found to provide up to an 80% protection from death, a considerable improvement over that found previously with nitrogen-containing bisphosphonates. This effect may originate in the much higher therapeutic indices of these alkyl bisphosphonates, as deduced from in vitro assays using LD_{50} values for growth inhibition of a human cell line. Overall, these results indicate that alkyl bisphosphonates are promising compounds for further development as agents against *Toxoplasma gondii* growth, in vivo.

Introduction

Toxoplasmosis, caused by the protozoan parasite *Toxoplasma gondii*, is a widespread disease affecting primarily immunocompromised and pregnant individuals. The standard therapy is a combination of pyrimethamine and sulfadiazine. However, many individuals do not tolerate sulfa drugs, so alternative regimens, such as clindamycin and pyrimethamine, may be necessary, and in less developed areas, less expensive drugs are required. One possible class of inexpensive, easy to prepare drugs are bisphosphonates, which we have found inhibit *T. gondii* growth, both in vitro[1] and in vivo.[2] Bisphosphonates are used extensively to treat bone resorption diseases,[3] and more recently they have been identified as potent antiparasitic agents.[1,2,4−8] The target of these drugs is generally the mevalonate or isoprenoid biosynthesis pathway, in particular the enzyme farnesyl pyrophosphate synthase (FPPS).[9−14] Inhibition of this enzyme results in inhibition of the formation of dolichols, ubiquinones and sterols, together with the inhibition of protein prenylation. In addition to these effects, some bisphosphonates also expand $\gamma\delta$ T cell populations[15,16] and have been shown to have potent antitumor[17−19] as well as antibacterial[20] activity.

In this paper, we investigate the activity of 60 bisphosphonates on the in vitro proliferation of *T. gondii*

* To whom correspondence should be addressed. Telephone: (217) 333-3374. Fax: (217) 244-0997. E-mail: eo@chad.scs.uiuc.edu.
‡ Department of Pathobiology and Center for Zoonoses Research, University of Illinois at Urbana-Champaign.
|| Department of Biophysics, University of Illinois at Urbana-Champaign.
§ Department of Chemistry, University of Illinois at Urbana-Champaign.
† Palo Alto Medical Foundation.
⊥ Present address: Center for Tropical and Global Emerging Infectious Diseases and Department of Cellular Biology, University of Georgia, Athens, GA 30602. Telephone: (706) 542-4736. E-mail: smoreno@cb.uga.edu.

10.1021/jm040132t CCC: $30.25 © 2005 American Chemical Society
Published on Web 04/02/2005

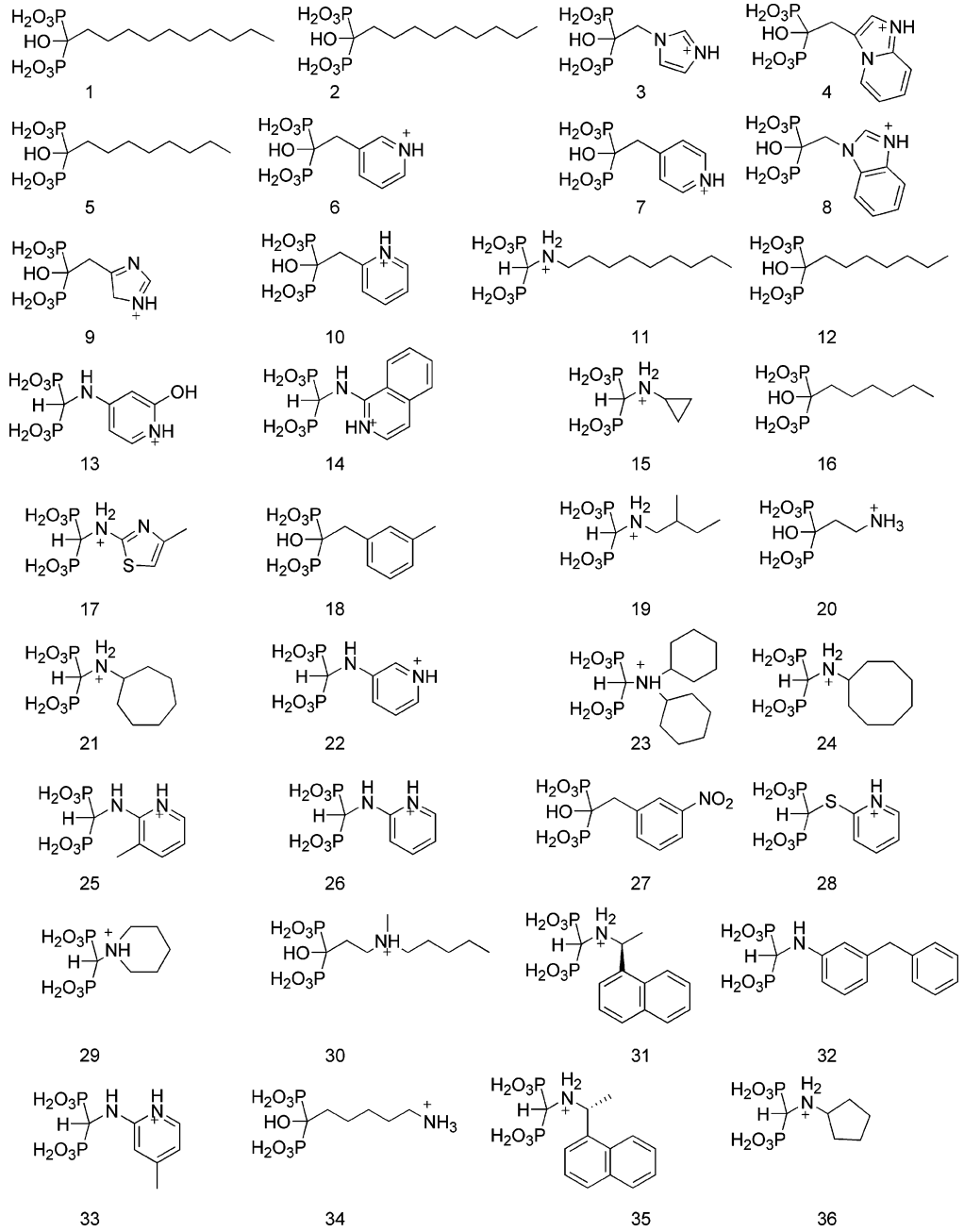

Figure 1. Structures of bisphosphonates in order of decreasing activity.

and use three-dimensional quantitative structure−activity relationship (3D-QSAR) techniques to analyze the results. We then test the three most active species in vivo in a mouse model. In addition, since the *T. gondii* genome contains a sequence for the enzyme 1-deoxyxylulose-5-phosphate reductoisomerase,[21] which is potently inhibited by fosmidomycin,[22,23] we also test the ability of fosmidomycin to inhibit *T. gondii* replication, in vitro.

Experimental Section

Bisphosphonates. The synthesis of most of the bisphosphonates investigated (Figures 1 and 2) have been described previously[1,4,16,24−26] and basically involves either the reductive phosphonylation of a carboxylic acid, for example:

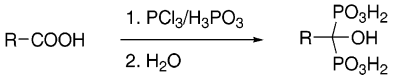

or condensation of an amine with triethylorthocarbonate and diethyl phosphite, followed by hydrolysis:

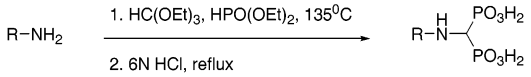

All compounds not reported previously (**31, 32, 35, 37, 41, 53, 55, 57**−**59**), with the exceptions noted below, had experimental H/C/N analyses that agreed within 0.4% of the calculated values. (**37**) Anal. ($C_{12}H_{13}O_7P_2Na$) C: calcd, 40.70; found, 40.24. (**59**) Anal. ($C_{14}H_{18}N_2O_6P_2 \cdot H_2O$) H calcd, 5.17; found, 4.64.

In Vitro Testing against *T. gondii* Proliferation. *T. gondii* tachyzoites of the 2F clone expressing β-galactosidase were a gift from Dr. L. David Sibley[27] and were routinely maintained in vitro in human foreskin fibroblast monolayers (HFF) in Dulbecco's modified Eagle's medium (DMEM) supplemented with 10% fetal bovine serum, 2 mM glutamine, 1 mM pyruvate, at 37 °C in a humid 5% CO_2 atmosphere. For in vitro

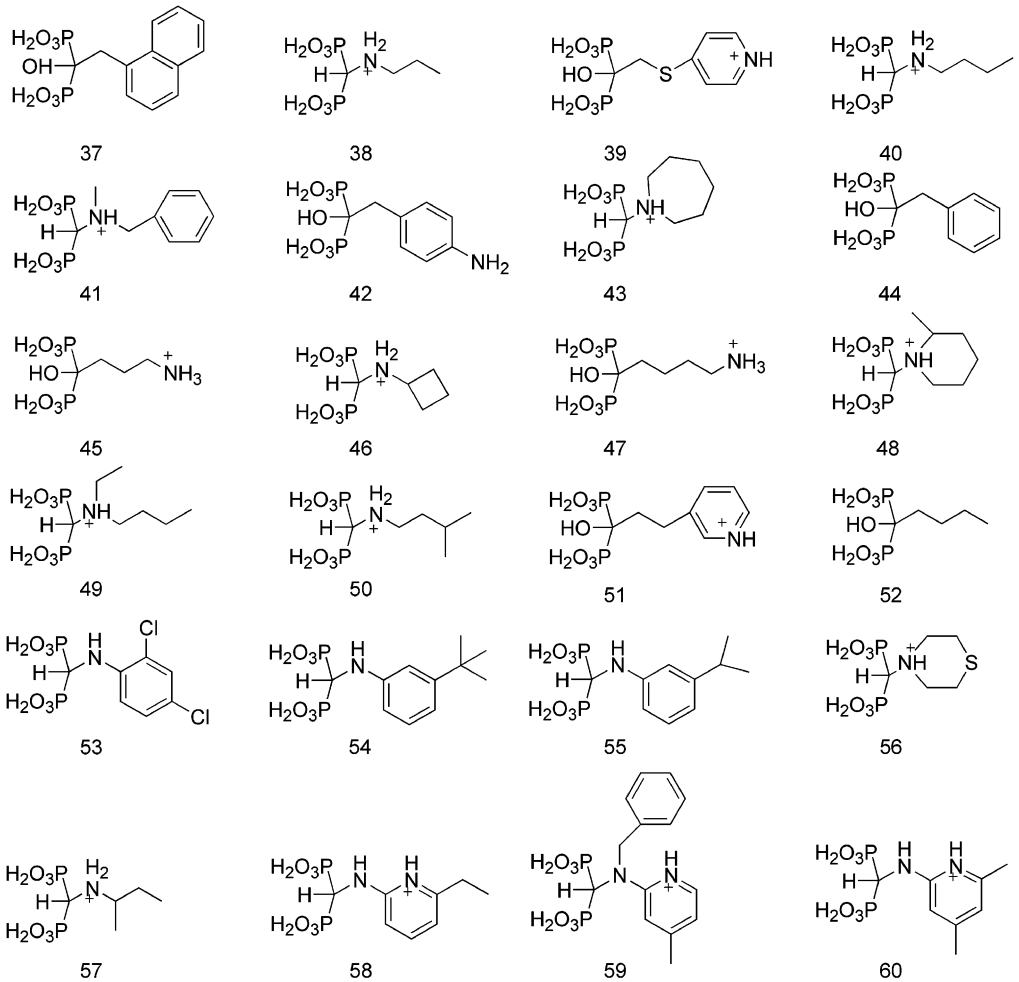

Figure 2. Structures of bisphosphonates in order of decreasing activity (continuation from Figure 1).

testing, confluent HFF monolayers grown in 96-well plates were used and the bisphosphonates dissolved in the same medium and serially diluted in the plates. Freshly isolated tachyzoites were filtered through a 3 μm filter and passed through a 22 gauge needle, before use. The cultures were inoculated with 10^4 tachyzoites per milliliter in the same media. The plates were incubated for 48 h at 37 °C, at which time they were centrifuged at 2500 rpm for 10 min, and the supernatant removed. At this time, 50 μL of lysis buffer (100 mM HEPES, pH 8.0, 1 mM $MgSO_4$, 1% Triton X-100 and 5 mM DTT) was added and the plate incubated at 50 °C for 30 min. At the end of the lysis period, 160 μL of assay buffer (100 mM sodium phosphate, pH 7.3, 102 μM β-mercaptoethanol and 9 mM $MgCl_2$) was added and the plates incubated for an additional 5 min at 37 °C. Subsequentially, 40 μL of a 6.25 mM solution of chlorophenol red-β-D-galactopyranoside (CPRG) substrate was added and the reaction continued at 37 °C for 10−30 min. The plates were read at 570 nm by using a microtiter plate reader.

For the calculation of the IC_{50}, the % of growth inhibition was plotted as a function of drug concentration by fitting the values to the rectangular hyperbolic function:

$$I = \frac{I_{max}C}{IC_{50} + C} \quad (1)$$

where I is the percent inhibition, $I_{max} = 100\%$ inhibition, C is the concentration of the inhibitor, and IC_{50} is the concentration for 50% growth inhibition. The regression analyses were performed by using Sigma Plot 5.0.[28]

Construction of *T. gondii* Overexpressing FPPS. The *TgFPPS* ORF (Ling et al., unpublished) was introduced into the expression vector ptubP30-FLAG/sag-CAT, replacing the P30 gene, to produce the plasmid ptubTgFPPS-FLAG/sag-CAT. *T. gondii* tachyzoites of the 2F clone[27] were transfected with 50 μg of the described plasmid, using basic electroporation protocols.[29] After electroporation, parasites were allowed to recover for 15 min, then inoculated into HFF cells in 25 cm^2 tissue culture flasks. Stable transformants were selected with 20 μM chloramphenicol and cloned by limited dilution in 96-well plates. The isolated clone was analyzed further by Western blots and immunofluorescence (Ling et al., unpublished). On the basis of the Western blot results, there was a 4−5-fold increase in the FPPS levels in the overexpressing strain.

In Vivo Testing. For the in vivo *Toxoplasma gondii* assays, tissue cysts of strain C56 were obtained as described previously.[30] Female Swiss Webster mice were infected orally with five cysts. Bisphosphonates were dissolved in phosphate-buffered saline (PBS) containing approximately 20% DMSO, at pH 6.8, and were delivered intraperitoneally (i.p.). The controls were infected mice treated with the drug diluent (PBS with approximately 20% DMSO). Treatment was initiated 3 days after infection and administered once a day via i.p. injection, for 10 days.

Computational Aspects. The structures of the bisphosphonate inhibitors shown in Figures 1 and 2 were built by using the Sybyl 6.9 Molecular Modeling program[31] running on an AMD based computer operating under Redhat Linux 8.0. Energy minimizations and geometry optimizations were performed on each molecule until the change in energy was less than 0.001 kcal. The force-field employed was the standard Tripos force-field[32] with default parameters. The minimization protocol consisted of three steps, starting with a steepest descent trajectory, followed by Powell minimization[33] and

finishing with the Broyden, Fletcher, Goldfarb and Shanno (BFGS) method.[34] Partial atomic charges were calculated by using the Gasteiger−Marsili protocol.[35] As described in previous work,[25] we used monoanionic (−P(O)(OH)(O⁻)) phosphonate groups. All side chains containing basic groups were protonated, again as described previously with our investigations of FPPS inhibition (and $\gamma\delta$ T cell activation) by bisphosphonates.[16,24,25,36] The molecules were then aligned by using the Align Database function in Sybyl. Two aligments were investigated. In the first, we used the most active compound (**1**) in its all-trans conformation as a template. Then, we used a second alignment, based on the X-ray diffraction determined conformation of farnesyl pyrophosphate in an avian FPPS,[37] to test to what extent small side chain "bends" might affect the QSAR results. In our previous QSAR study of bisphosphonates active in bone resorption, this curvature was found to improve the results for very long aryl−alkyl bisphosphonates.[36]

For the QSAR calculations, molecules were placed in a rectangular grid having a 2.00 Å spacing. We then used standard Sybyl parameters for a partial least squares (PLS) analysis. The number of components in the PLS models were optimized by using q^2, obtained from the leave-one-out cross validation procedure, with the SAMPLS[38] sampling method. The number of components was increased until additional components did not increase q^2 by at least 5% per added component. For both the comparative molecular field analysis (CoMFA, ref 39) and the comparative molecular similarity analysis (CoMSIA, ref 40) in the all-trans alignment, two components were found to be optimal and were therefore used to generate the QSAR models. The CoMFA models were generated by using steric and electrostatic probes with standard 30 kcal/mol cutoffs.[39] In the CoMSIA analyses, again only steric and electrostatic probes were used to generate the QSAR models, using a 0.3 attenuation factor.[40] Four validation test sets were generated by randomly removing five different compounds from the initial training sets. The QSAR models were then recomputed for each of these test sets and activities of the test set compounds ($N = 4 \times 5$=20) predicted by using both CoMFA and CoMSIA.

Results and Discussion

We show in Figures 1 and 2 the structures of the 60 bisphosphonates investigated, ordered by decreasing activity. Growth inhibition tests were all carried out in quadruplicate and the average IC_{50} results for each compound are presented in Tables 1 and 2, together with the corresponding pIC_{50} values, defined as:

$$pIC_{50} = -\log_{10} [IC_{50}, M] \quad (2)$$

The overall range in activity found was from 280 nM (**1**) to 235 μM (**60**). For the top 10 most active compounds, the IC_{50} values were all <10 μM (Tables 1, 2). Most of these compounds (seven out of ten) are nitrogen-containing bisphosphonates, which we have found previously are potent inhibitors of the growth of parasitic protozoa such as *Trypanosoma cruzi*,[1,7,8] *Trypanosoma brucei*[1,4] and *Leishmania donovani*,[1,2] and several of them are currently in clinical use. For example, **3** is zoledronate; **4** is minodronate and **6** is risedronate. Each of these nitrogen-containing bisphosphonates is a potent inhibitor of the FPPS enzyme.[9−14,25,41] What is surprising about these results, however, is that three of the five most potent *T. gondii* growth inhibitors, **1**, **2**, and **5**, do not contain a positively charged nitrogen center. This raises the question as to whether FPPS inhibition is involved in *T. gondii* growth inhibition. Here, it would be of interest to investigate the inhibition of a pure, expressed *T. gondi* FPPS, but so far, we did not succeed in obtaining a stable, isolated protein. However, we can investigate the correlation between *T. gondi* growth inhibition and FPPS inhibition using other FPPS enzymes, such as those from *Leishmania major*[25] and humans.[10] The results of these correlations are shown in Figure 3A (bottom two data sets) for four nitrogen-containing bisphosphonates known to be potent FPPS inhibitors and which are currently used to treat certain bone resorption diseases: zoledronate (**3**), minodronate (**4**), risedronate (**6**) and pamidronate (**20**). As can be seen in Figure 3A, the correlations between *T. gondii* growth inhibition and FPPS inhibition are high for both FPPS systems ($R^2 = 0.948-0.968$), supporting an FPPS target in *T. gondi*. We also find for the six alkyl bisphosphonates that there is, once again, a correlation between the *T. gondii* IC_{50} and, in this case, *L. major* FPPS inhibition (Figure 3A). The observation that all these alkyl bisphosphonates are located on a line above that seen with the N-containing bisphosphonates suggests that the alkyl bisphosphonates have better transport properties, since they would otherwise be less effective than, for example, zoledronate.

To further test the hypothesis that the alkyl bisphosphonates do in fact function by inhibiting FPPS, we constructed a *T. gondii* strain which overexpresses this enzyme (Ling et al., unpublished). If FPPS is indeed the target for these compounds, we would expect that higher levels of bisphosphonate would be required in order to obtain 50% growth inhibition. Plus, the increase in IC_{50} for the alkyl bisphosphonates should be the same as that seen with the potent nitrogen-containing bisphosphonate inhibitors, which are known to function by inhibiting FPPS. The IC_{50} values found with the wild type and the FPPS overexpressing strain are shown in Table 3. Here, we show results for the three most potent alkyl bisphosphonates (**1**, **2**, **5**) together with control results for the nitrogen containing bisphosphonate zoledronate (**3**) and for atovaquone (566C80), a potent *T. gondii* growth inhibitor not involved in FPPS inhibition.[42] As can be seen from the results shown in Table 3, the increase in IC_{50} for the alkyl bisphosphonates varies from 2.4 to 6.1×, to be compared with ∼10× for zoledronate, in the FPPS-overexpressing strain. On the other hand, the IC_{50} values we find with atovaquone in our assay are 290 nM in wild type *T. gondii* and 280 nM in *T. gondii* overexpressing FPPS, Table 3. While the origins of the deviations seen with the alkyl and N-containing bisphosphonates are not clear, these results nevertheless support the idea that FPPS is a major target for all bisphosphonates in *T. gondii* growth inhibition and strongly support the correlations between FPPS inhibition and *T. gondi* growth shown in Figure 3A.

For the alkyl bisphosphonates, there appears to be a rather monotonic increase in activity as the length of the alkyl side-chain increases (Tables 1, 3), in that the pattern of activity **1** > **2** > **5** correlates in a general way with the chain length decrease, from 10 (**1**) to 9 (**2**) to 8 (**5**) carbons. In fact, this decrease in activity continues out through 4 carbons (**53**) and as shown graphically in Figure 3B, there is an exponential relationship between IC_{50} and chain length between 4 and 10 carbon atoms ($R^2 = 0.99$). This is basically the same behavior as that reported previously with *Entamoeba histolytica*, *Plas-*

Table 1. Experimental (IC_{50} and pIC_{50}) and Predicted CoMFA and CoMSIA (pIC_{50}) Results for Bisphosphonate Inhibition of *Toxoplasma gondii* Growth and Related Statistics [all-trans model]

	exp. activity		CoMFA predicted pIC_{50}					CoMSIA predicted pIC_{50}				
cpd	IC_{50}[a]	pIC_{50}	TS[b]	four-compound test set				TS[b]	four-compound test set			
1	0.28	6.55	5.72	6.13	5.83	5.77	6.16	5.87	5.91	5.99	5.93	5.95
2	0.55	6.26	5.61	6.01	5.72	5.66	6.04	5.65	5.68	5.76	5.70	5.73
3	0.79	6.10	5.31	5.39	5.27	5.30	**4.98**	5.44	5.44	5.41	5.43	**5.16**
4	1.88	5.73	5.38	**5.06**	5.37	5.37	5.21	5.46	**5.34**	5.44	5.43	5.28
5	2.38	5.62	5.28	5.58	5.37	5.31	5.57	5.32	5.34	5.41	5.35	5.39
6	2.40	5.62	5.34	5.23	5.28	5.32	**4.96**	5.49	5.46	5.46	5.48	**5.23**
7	3.50	5.46	5.35	5.27	**5.26**	5.30	5.00	5.37	5.37	**5.31**	5.33	5.15
8	4.50	5.35	5.39	5.15	5.38	5.38	5.18	5.46	5.36	5.44	5.44	5.27
9	6.70	5.17	5.23	5.25	5.19	5.21	5.00	5.34	5.33	5.31	5.32	5.08
10	8.11	5.09	5.21	5.06	5.18	5.22	4.89	5.27	5.24	5.26	5.28	5.06
11	8.89	5.05	5.70	6.12	5.83	5.77	6.15	5.67	5.70	5.80	5.76	5.75
12	13.80	4.86	4.79	4.95	4.85	4.80	4.92	4.93	4.95	4.99	4.94	5.00
13	17.40	4.76	4.30	4.43	4.27	**4.19**	4.42	4.08	4.10	4.07	**3.97**	4.08
14	20.89	4.68	4.00	4.26	3.98	3.95	4.34	4.01	4.01	4.02	3.95	4.05
15	23.08	4.64	4.20	4.16	4.20	4.24	4.15	4.20	4.22	4.20	4.25	4.17
16	25.31	4.60	4.47	4.54	**4.50**	4.45	4.48	4.57	4.59	**4.61**	4.57	4.63
17	30.92	4.51	4.68	4.41	4.65	4.65	4.42	4.49	4.49	4.45	4.51	4.48
18	36.42	4.44	4.66	4.21	4.61	4.61	4.17	4.62	4.59	4.56	4.57	4.63
19	36.60	4.44	4.06	4.17	4.08	4.04	4.22	4.04	4.04	4.06	4.06	4.09
20	38.00	4.42	4.38	4.33	4.39	4.39	4.19	4.28	4.29	4.34	4.28	4.15
21	39.65	4.40	4.09	4.13	4.10	**4.05**	4.17	4.12	4.08	4.13	4.10	4.20
22	41.95	4.38	4.30	4.39	4.26	4.22	4.35	4.14	4.16	4.11	4.04	4.12
23	42.05	4.38	4.11	4.23	4.12	4.15	4.23	4.11	4.11	4.14	4.16	4.06
24	43.22	4.36	4.11	4.15	4.13	4.07	4.32	4.05	3.98	4.07	4.02	4.18
25	44.48	4.35	4.10	4.26	4.08	4.04	4.28	4.04	4.05	4.03	3.97	4.02
26	44.63	4.35	4.21	4.28	4.19	**4.14**	4.25	4.19	4.21	4.18	**4.12**	4.15
27	47.90	4.32	4.69	4.25	4.64	4.65	4.22	4.68	4.66	4.64	4.63	4.66
28	51.19	4.29	4.92	**4.88**	4.85	4.86	4.57	4.75	**4.83**	4.70	4.68	4.62
29	51.22	4.29	3.97	3.92	**4.01**	4.06	3.94	4.14	4.12	**4.16**	4.23	4.10
30	54.92	4.26	4.76	4.77	**4.89**	4.80	4.69	4.81	4.81	**5.00**	4.82	4.79
31	55.06	4.26	4.15	4.20	4.14	4.17	4.29	4.12	4.18	4.12	4.15	4.09
32	56.16	4.25	3.74	**3.87**	3.74	3.71	4.06	3.88	**3.89**	3.90	3.83	4.02
33	59.04	4.23	4.10	4.22	4.09	4.04	4.20	4.12	4.13	4.12	4.05	4.13
34	59.70	4.22	4.76	**4.86**	4.78	4.72	4.54	4.30	**4.36**	4.33	4.26	4.31
35	63.23	4.20	4.30	4.28	4.28	4.32	4.23	4.40	4.45	4.37	4.42	4.33
36	68.43	4.16	4.14	4.07	4.14	4.15	4.09	4.12	4.09	4.12	4.13	4.15
37	68.75	4.16	3.97	4.09	3.97	3.95	4.18	4.16	4.16	4.15	4.13	4.25
38	69.25	4.16	4.18	4.10	4.20	4.18	**4.07**	4.12	4.15	4.13	4.16	**4.11**
39	72.52	4.14	4.06	4.12	4.08	4.08	4.13	3.72	3.72	3.74	3.72	3.71
40	76.14	4.12	4.14	4.12	4.17	4.14	4.11	4.11	4.13	4.14	4.15	4.15
41	76.70	4.12	3.89	3.90	3.91	3.92	3.92	3.92	3.90	3.94	3.96	3.98
42	80.34	4.10	4.62	4.23	4.56	4.57	4.08	4.60	4.61	4.55	4.55	4.58
43	89.77	4.05	4.15	3.99	4.20	4.22	4.14	4.22	4.17	4.24	4.29	4.19
44	90.23	4.04	4.62	4.26	4.57	4.59	4.10	4.62	4.63	4.56	4.59	4.59
45	108.80	3.96	4.54	4.47	4.53	4.51	4.31	4.40	4.41	4.43	4.35	4.26
46	120.90	3.92	4.06	3.98	4.07	**4.10**	4.03	4.12	4.10	4.12	**4.15**	4.11
47	126.40	3.90	4.47	4.44	4.47	4.43	4.25	3.98	4.01	4.01	3.92	3.94
48	131.60	3.88	3.97	3.89	**4.03**	4.04	4.02	4.03	4.00	**4.06**	4.10	4.01
49	132.00	3.88	4.08	3.98	4.08	4.09	4.06	4.02	3.97	4.02	4.03	4.07
50	135.00	3.87	4.17	4.21	4.19	4.15	**4.25**	4.09	4.09	4.12	4.11	**4.17**
51	147.30	3.83	3.90	3.95	3.90	3.92	3.93	3.68	3.68	3.72	3.66	3.69
52	149.70	3.82	4.14	4.01	4.14	4.12	3.97	4.31	4.33	4.30	4.30	4.30
53	153.50	3.81	3.84	3.88	3.82	3.76	4.00	4.05	4.04	4.02	3.98	4.10
54	156.60	3.81	3.66	3.87	3.65	3.63	**4.04**	3.94	3.91	3.96	3.90	**4.15**
55	160.40	3.79	3.45	3.54	3.43	3.42	3.69	3.78	3.75	3.78	3.74	3.96
56	160.80	3.79	4.07	4.01	4.10	**4.17**	3.98	4.24	4.24	4.25	**4.34**	4.18
57	164.30	3.78	4.15	4.15	4.16	4.16	4.13	4.12	4.13	4.13	4.15	4.11
58	217.70	3.66	4.44	4.52	4.44	4.36	4.46	4.44	4.45	4.46	4.36	4.47
59	226.40	3.65	3.80	3.84	3.78	3.76	3.87	3.69	3.66	3.69	3.62	3.75
60	234.70	3.63	4.10	4.10	4.07	4.02	4.09	4.08	4.08	4.09	4.00	4.12
R^2			0.69	0.78	0.69	0.71	0.78	0.73	0.73	0.74	0.76	0.70
Q^2			0.55	0.57	0.54	0.57	0.51	0.61	0.58	0.61	0.65	0.53
F[c]			62.2	60.2	59.0	62.7	59.0	76.1	70.9	73.1	82.4	61.8
n[d]			2	3	2	2	3	2	2	2	2	2
N[e]			60	55	55	55	55	60	55	55	55	55
%S[f]			0.708	0.667	0.713	0.710	0.672	0.573	0.598	0.578	0.570	0.607
%E[g]			0.292	0.333	0.287	0.290	0.328	0.427	0.402	0.422	0.430	0.393
R[h]				0.455	0.273	0.340	0.496		0.286	0.241	0.421	Row700.403
$\bar{R}_i$[i]					**0.391**					**0.337**		

[a] IC_{50} reported in μM. [b] TS = Training set, all 60 compounds. [c] F-test, calculated by Sybyl. [d] n denotes the number of components or features used as descriptors in the model. [e] N denotes the number of compounds used to generate the model. [f] %S denotes the steric contribution to the model. [g] %E denotes the electrostatic contribution to the model. [h] R is the residual (pIC_{50}) over the test set. [i] $\bar{R}_i$ The bolded value under the training set (TS) is the average value of the residual over all of the test sets.

modium falciparum and *T. brucei* growth inhibition[4,26] where we found that activity peaked at about a C_{10} carbon side-chain length, then decreased with increasing chain length, due most likely to steric repulsions

Table 2. Experimental (IC_{50} and pIC_{50}) and Predicted CoMFA and CoMSIA (pIC_{50}) Results for Bisphosphonate Inhibition of *Toxoplasma gondii* Growth and Related Statistics [FPP-based alignment]

	exp. activity		CoMFA predicted pIC_{50}					CoMSIA predicted pIC_{50}				
cpd	IC_{50}[a]	pIC_{50}	TS[b]	four-compound test set				TS[b]	four-compound test set			
1	0.28	6.55	6.48	6.41	6.54	6.45	6.44	6.20	6.11	6.19	6.26	5.88
2	0.55	6.26	6.12	6.03	6.16	6.04	6.03	5.87	5.80	5.87	5.92	5.66
3	0.79	6.10	5.84	5.66	5.76	5.56	**5.14**	5.21	5.33	5.15	5.20	**4.79**
4	1.88	5.73	5.45	**5.32**	5.41	5.46	5.43	5.26	**5.21**	5.26	5.27	4.93
5	2.38	5.62	5.68	5.59	5.71	5.57	5.55	5.39	5.35	5.41	5.43	5.34
6	2.40	5.62	5.48	5.46	5.32	5.34	**5.08**	5.24	5.38	5.20	5.24	**4.90**
7	3.50	5.46	5.29	5.34	**5.06**	5.18	4.97	4.94	5.13	**4.86**	4.90	4.74
8	4.50	5.35	5.44	5.33	5.42	5.46	5.41	5.28	5.22	5.29	5.30	4.91
9	6.70	5.17	5.32	5.31	5.27	5.18	4.97	5.09	5.24	5.03	5.07	4.75
10	8.11	5.09	5.21	5.08	5.17	5.07	4.92	5.13	5.22	5.13	5.13	4.87
11	8.89	5.05	5.13	5.48	5.26	5.55	5.61	6.04	5.96	6.03	6.06	5.86
12	13.80	4.86	4.60	4.65	4.59	4.59	4.57	4.83	4.82	4.87	4.85	4.96
13	17.40	4.76	4.40	4.28	4.36	**3.96**	4.22	4.38	4.38	4.41	**4.10**	4.06
14	20.89	4.68	4.63	4.80	4.61	4.83	4.85	4.33	4.25	4.40	4.35	3.83
15	23.08	4.64	4.44	4.28	4.53	4.34	4.29	4.12	4.18	4.09	4.14	4.17
16	25.31	4.60	4.33	4.37	**4.28**	4.23	4.23	4.43	**4.45**	4.45	4.43	4.63
17	30.92	4.51	4.29	4.35	4.31	4.43	4.42	4.15	4.19	4.10	4.16	4.46
18	36.42	4.44	4.16	4.31	4.15	4.40	4.44	4.22	4.15	4.19	4.24	4.40
19	36.60	4.44	3.99	3.84	3.99	3.89	4.01	4.15	4.16	4.20	4.16	4.43
20	38.00	4.42	4.41	4.41	4.37	4.37	4.25	4.32	4.49	4.34	4.29	4.17
21	39.65	4.40	4.27	4.08	4.26	**3.98**	4.18	4.01	3.96	4.01	**3.88**	4.29
22	41.95	4.38	4.39	4.31	4.35	4.04	4.21	4.34	4.36	4.34	4.10	4.03
23	42.05	4.38	4.38	4.36	4.52	4.27	4.33	4.11	4.13	4.12	4.12	4.28
24	43.22	4.36	4.31	4.11	4.31	4.03	4.18	4.00	3.89	4.02	3.87	4.24
25	44.48	4.35	4.51	4.54	4.57	4.45	4.54	4.31	4.28	4.36	4.24	3.89
26	44.63	4.35	4.26	4.16	4.24	**3.96**	4.13	4.25	4.28	4.27	**4.06**	4.04
27	47.90	4.32	4.32	4.40	4.31	4.52	4.55	4.34	4.30	4.32	4.34	4.47
28	51.19	4.29	4.89	**5.37**	4.80	5.02	4.80	5.03	**5.26**	5.00	5.02	4.81
29	51.22	4.29	4.05	4.17	**4.18**	4.27	4.11	4.17	4.18	**4.19**	4.28	4.16
30	54.92	4.26	4.19	4.39	**4.76**	4.29	4.39	4.79	4.72	**5.05**	4.71	4.72
31	55.06	4.26	4.28	4.22	4.27	4.23	4.14	4.05	4.09	4.05	4.07	4.35
32	56.16	4.25	4.41	**3.79**	4.26	3.95	3.90	3.71	**3.66**	3.69	3.73	3.90
33	59.04	4.23	4.05	4.04	4.03	3.93	4.04	4.18	4.16	4.20	4.00	4.04
34	59.70	4.22	4.20	**4.97**	4.09	4.35	4.27	4.51	**4.82**	4.45	4.47	4.74
35	63.23	4.20	4.22	4.37	4.23	4.41	4.30	4.14	4.10	4.18	4.25	4.28
36	68.43	4.16	4.43	4.22	4.46	4.26	4.24	4.03	4.00	4.03	3.98	4.19
37	68.75	4.16	4.16	4.34	4.24	4.48	4.60	4.33	4.19	4.35	4.39	4.47
38	69.25	4.16	3.93	3.82	3.92	3.87	**3.91**	4.06	4.10	4.04	4.06	**4.26**
39	72.52	4.14	3.82	4.04	3.81	4.01	3.96	3.99	3.98	4.00	4.12	3.81
40	76.14	4.12	3.88	3.80	3.82	3.80	3.90	4.12	4.16	4.12	4.09	4.42
41	76.70	4.12	4.03	4.16	4.08	4.21	4.17	4.24	4.17	4.27	4.39	4.11
42	80.34	4.10	4.28	4.54	4.28	4.45	4.36	4.39	4.40	4.38	4.40	4.56
43	89.77	4.05	3.81	3.98	4.03	4.09	3.97	4.17	4.12	4.22	4.28	4.20
44	90.23	4.04	4.37	4.41	4.31	4.39	4.35	4.22	4.24	4.17	4.23	4.37
45	108.80	3.96	4.34	4.34	4.25	4.25	4.15	4.56	4.66	4.54	4.45	4.37
46	120.90	3.92	4.26	4.10	4.32	**4.23**	4.20	4.08	4.09	4.07	**4.08**	4.15
47	126.40	3.90	4.34	4.56	4.17	4.32	4.27	4.73	4.94	4.68	4.67	4.68
48	131.60	3.88	4.07	4.18	**4.42**	4.28	4.17	4.12	4.11	**4.17**	4.21	4.11
49	132.00	3.88	3.64	3.73	3.67	3.77	3.80	3.91	3.91	3.91	3.94	4.20
50	135.00	3.87	3.94	3.78	3.93	3.75	**3.93**	4.07	4.07	4.09	3.99	**4.42**
51	147.30	3.83	3.73	3.99	3.76	3.98	3.99	4.13	4.08	4.20	4.23	3.89
52	149.70	3.82	4.10	3.91	4.01	3.97	3.96	4.12	4.12	4.09	4.14	4.20
53	153.50	3.81	3.91	3.74	3.88	3.74	3.88	3.96	3.93	3.94	3.92	3.95
54	156.60	3.81	3.93	3.96	3.89	4.06	**4.24**	3.84	3.70	3.83	3.88	**4.06**
55	160.40	3.79	3.74	3.62	3.61	3.71	3.78	3.68	3.59	3.66	3.71	3.88
56	160.80	3.79	3.97	4.10	4.09	**4.21**	4.04	4.16	4.19	4.14	**4.27**	4.20
57	164.30	3.78	4.29	4.18	4.26	4.22	4.14	4.13	4.13	4.09	4.10	4.31
58	217.70	3.66	3.97	4.14	3.97	3.91	4.16	4.44	4.42	4.48	4.19	4.32
59	226.40	3.65	3.51	3.63	3.53	3.65	3.60	3.84	3.80	3.88	3.81	3.69
60	234.70	3.63	4.06	4.08	4.01	3.89	4.04	4.15	4.12	4.17	3.95	3.99
R^2			0.88	0.84	0.89	0.84	0.82	0.70	0.72	0.70	0.72	0.59
Q^2			0.54	0.56	0.56	0.54	0.42	0.43	0.46	0.43	0.46	0.34
F[c]			78.93	69.15	75.90	67.48	56.45	42.84	44.30	40.27	44.63	36.67
n[d]			5	4	5	4	4	3	3	3	3	2
N[e]			60	55	55	55	55	60	55	55	55	55
$\%S$[f]			0.631	0.647	0.647	0.663	0.690	0.562	0.604	0.559	0.584	0.693
$\%E$[g]			0.369	0.353	0.353	0.337	0.310	0.438	0.396	0.441	0.416	0.307
R[h]				0.540	0.374	0.467	0.447		0.535	0.384	0.422	0.586
$\bar{R}_i$[i]					**0.457**					**0.481**		

[a] IC_{50} reported in μM. [b] TS = Training set, all 60 compounds. [c] F-test, calculated by Sybyl. [d] n denotes the number of components or features used as descriptors in the model. [e] N denotes the number of compounds used to generate the model. [f] $\%S$ denotes the steric contribution to the model. [g] $\%E$ denotes the electrostatic contribution to the model. [h] R is the residual (pIC_{50}) over the test set. [i] $\bar{R}_i$ The bolded value under the training set (TS) is the average value of the residual over all of the test sets.

with bulky aromatic groups in the FPPS active site, which control chain elongation.[37] Since longer chains were found to decrease activity in all three previous in vitro assays, we did not test longer chain compounds in

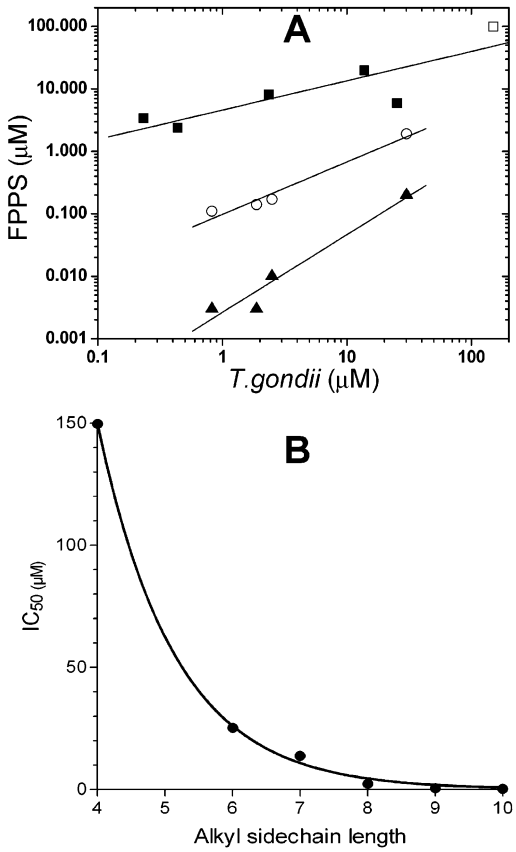

Figure 3. *T. gondii* growth inhibition correlations. A, correlations between *T. gondi* IC_{50} values and FPPS inhibition for nitrogen-containing bisphosphonates in human FPPS (▲), *L. major* FPPS (○) and alkyl bisphosphonates in the *L. major* FPPS (■). The □ point represents a lower limit to the IC_{50} value in *L. major* FPPS. B, Dependence of bisphosphonate activity in in vitro *T. gondii* growth inhibition as a function of alkyl chain length.

Table 3. Effect of FPPS Overexpression in *T. gondii* on Growth Inhibition

drug	Wild-type *T. gondii* (IC_{50}, μM)	FPPS overexpressing *T. gondii* (IC_{50}, μM)
atovaquone	0.29 ± 0.11	0.28 ± 0.080
1	0.12 ± 0.030	1.1 ± 0.23
	0.30 ± 0.065	1.2 ± 0.28
	0.28 ± 0.020	1.7 ± 0.25
2	0.62 ± 0.12	1.9 ± 0.54
	0.15 ± 0.025	0.57 ± 0.094
	0.55 ± 0.060	1.7 ± 0.24
3 (zoledronate)	0.60 ± 0.16	7.8 ± 3.0
	1.1 ± 0.21	8.3 ± 1.9
	0.79 ± 0.28	7.8 ± 1.5
5	2.2 ± 0.47	3.3 ± 0.77
	2.5 ± 0.74	5.8 ± 1.7
	2.4±0.42	5.8 ± 1.1

T. gondii since it seems most likely that this pattern will again be reproduced.

Next, we consider the 3D-QSAR results for *T. gondii* growth inhibition since, clearly, there are a very large number of different structural features in **1**−**60**, necessitating a computational analysis. Here, as described above, we used both CoMFA and CoMSIA methods, on two different molecular alignments. In the first, Figure 4A, we aligned all molecules to the most stable, all-trans form of the most active species, **1**. In the second, Figure 4B, all molecules were aligned to FPP, extracted from the crystallographic structure of FPPS−FPP[37] (PDB File 1UBX). The CoMFA analysis using the all-trans alignment of **1** indicated that best results were obtained by using a two-component (steric plus electrostatic) model, having an R^2 of 0.686, a q^2 of 0.552 and an F-test value of 62.2, Table 1. The external validation procedure showed that these CoMFA models enabled prediction of *T. gondii* growth inhibition within a factor of about 2.5 (on average) over the range of activities seen experimentally, Table 1. Similar results were obtained with a two-component (steric plus electrostatic) CoMSIA model, which had an R^2 value of 0.728, a q^2 value of 0.608 and an F-test value of 76.2, Table 1. Application of the external validation procedure showed that these CoMSIA models had on average a residual pIC_{50} of 0.337, again enabling prediction of the activities of *T. gondii* growth inhibition within a factor of ∼2.2, Table 1. The results obtained by using the second, alternative alignment (based on the FPP−FPPS crystal structure, 1UBX) were generally similar and are shown in Table 2 and had average predictive errors of between 2.9 and 3.1.

The CoMSIA field results obtained by using the first alignment are shown in Figure 5. The colors represent the following: green, steric feature favored; yellow, steric feature disfavored; blue, positive charge favored; red, positive charge disfavored. Also shown are three bisphosphonates, superimposed on the CoMSIA fields: **1**, **6** (risedronate) and **37**. Results from the all-trans alignment are shown in A−C, and those from the FPP-based alignment are shown in D−F. As may be seen in Figure 5A,D **1** has good activity due to the presence of the long alkyl chain (green region), and as may be seen in Table 1, this steric interaction makes a major (∼60−70%) contribution to the QSAR models using both CoMFA and CoMSIA methods. For species such as risedronate (**6**), Figure 5B,E relatively good activity is obtained due to the presence of the positive charge feature located on the pyridine ring (blue feature). For species such as **37**, there are strong repulsive interactions (yellow region, steric interaction disfavored, Figure 5C,F) which decrease activity. The presence of these structural features can be correlated with the known crystal structures of FPPS. For example, the structures[37,43] of avian, *Escherichia coli* and *Staphylococcus aureus* FPPSs all contain a long, narrow, hydrophobic pocket (which contacts GPP) and correlates with the green steric features. Also, in the *E. coli* FPPS−risedronate−IPP structure,[43] there is an electrostatic interaction (hydrogen bond) between the protein and the risedronate nitrogen (blue feature). The hydrophobic pocket packs tightly around GPP (or FPP) in the avian FPPS complexes and would not permit binding of highly bulky species such as **23**, **37** or **59**. On the basis of these results, it can be seen that high activity is afforded either by the presence of a long alkyl chain (resulting in a favorable steric interaction) or by the presence of a suitably located positive charge feature.

In addition to these results on bisphosphonates, we tested the idea that another isoprene biosynthesis pathway inhibitor, fosmidomycin, might also inhibit the growth of *T. gondii*. The genome of *T. gondii* contains several enzymes of the non-mevalonate or methylerythritol phosphate (MEP) pathway.[21] One of the enzymes which has been identified (computationally) is 1-deoxyxylulose-5-phosphate reductoisomerase (DXR),[21] and

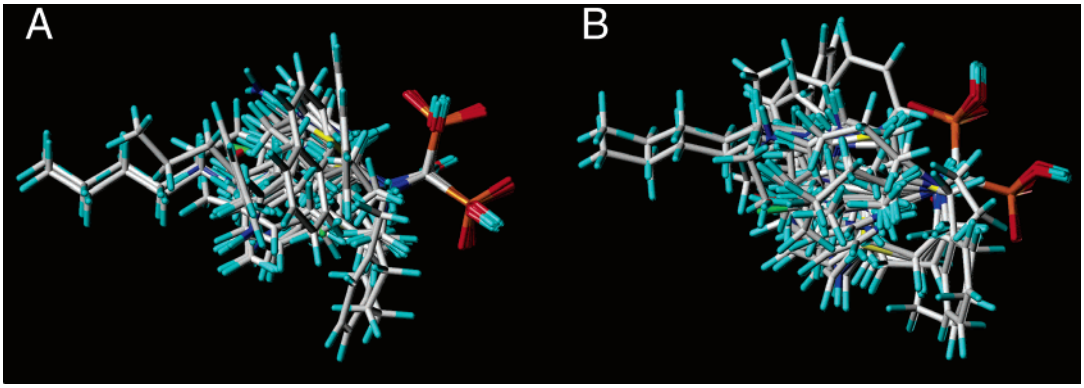

Figure 4. Molecular alignments used for CoMFA and CoMSIA analyses. A, based on **1** in the extended or all-trans form; B, based on the FPP side chain conformation in PDB File 1UBX.

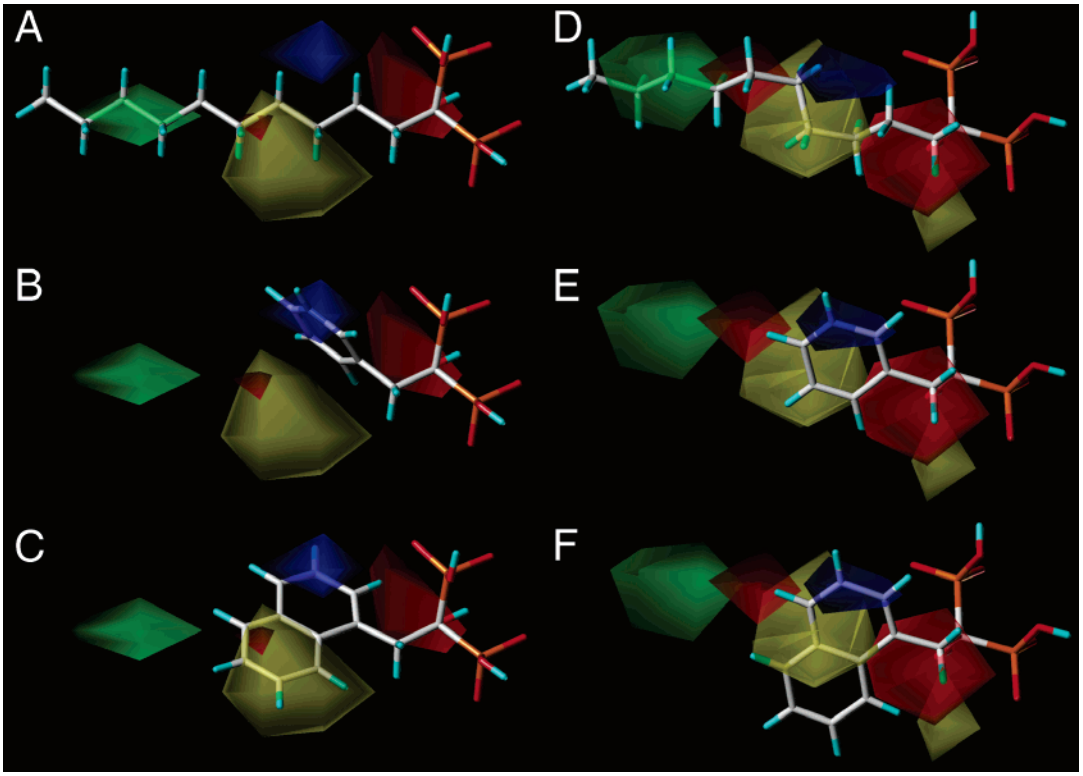

Figure 5. CoMSIA results showing steric and electrostatic fields. A−C obtained by using the all-trans alignment of **1**. D−F obtained by using the FPP-based alignment. Blue = positive charge desirable; red = positive charge not desirable; green = steric bulk favorable; yellow = steric bulk unfavorable. The most active compound, **1**, is shown in A, D; compound **6** (risedronate) is shown in B, E; and compound **37** is shown in C, F.

the DXRs of several species, including *Plasmodium falciparum* and *Pseudomonas aeruginosa*, have been found to be inhibited at <100 nM levels by the phosphonate drug fosmidomycin.[22,44] However, we found no inhibition of *T. gondii* growth by fosmidomycin, even at levels as high as 50 μM. This result is reminiscent of the failure of fosmidomycin to inhibit the growth of *Mycobacterium tuberculosis*[45] and several other species containing the MEP pathway, but at present whether in *T. gondii* this is due to poor transport, lack of expression of DXR, or to the presence of other isoprenoid biosynthesis pathways, is unknown.

In Vivo Results and Toxicity. Given that we now have numerous inhibitors of *T. gondii* growth in vitro, we consider the utility of these species in inhibiting *T. gondii* growth, in vivo. What is required, of course, is an inhibitor which is effective in inhibiting *T. gondii* growth without inhibiting host cell growth. For example, while **1** is very effective in controlling *T. gondii* growth in vitro, it would not be useful if it were toxic to human cells. To begin to assess the potential utility of the bisphosphonates shown in Figures 1 and 2, we used the "therapeutic index" (T.I.) method reported previously,[26] in which the T.I. is defined as:

$$\text{T.I.} = \frac{\text{LD}_{50}}{\text{IC}_{50}} \tag{3}$$

where LD_{50} represents the dose required to inhibit the growth of a human (KB, nasopharyngeal carcinoma) cell line by 50%, and the IC_{50} is as defined above, for *T. gondii* growth inhibition (eq 1). The IC_{50}, LD_{50} and T.I. results are shown in Table 4 and are presented graphically in Figure 6, where we show the T.I. plotted as a

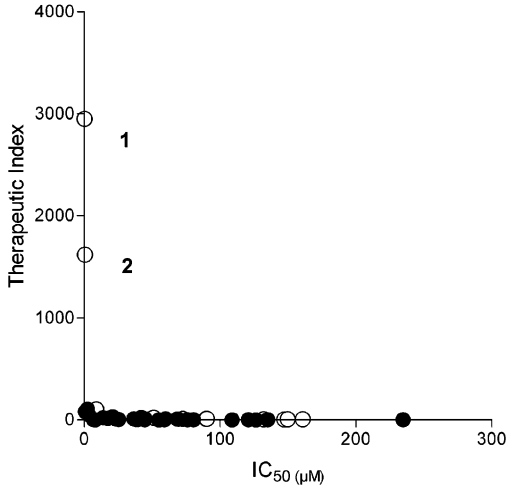

Figure 6. IC_{50} vs therapeutic index (LD_{50}/IC_{50}) results. Open circles indicate that the T.I. value is a lower limit (no KB cell inhibition noted at the highest level tested of 300 μg/mL). The LD_{50} results were from ref 26.

Table 4. Growth Inhibition (IC_{50}) Data for *Toxoplasma gondii*, Toxicity Data (LD_{50}) for a KB Cell Line and Computed Therapeutic Index (TI) Results for Bisphosphonate Inhibitors

cpd	IC_{50}[a]	LD_{50}[b]	TI[c]	cpd	IC_{50}[a]	LD_{50}[b]	TI[c]
1	0.28	>826	>2950.00	**29**	51.22	>1119	>21.85
2	0.55	>892	>1621.82	**30**	54.92	10.4	0.19
3	0.79	63.7	80.93	**33**	59.04	137	2.32
6	2.40	255	106.25	**34**	59.70	680	11.39
7	3.50	171	48.86	**36**	68.43	629	9.19
9	6.70	41	6.12	**38**	69.25	499	7.21
10	8.11	13.9	1.71	**39**	72.52	>746	>10.29
11	8.89	>919	>103.37	**40**	76.14	212	2.78
12	13.80	302	21.88	**42**	80.34	218	2.71
13	17.40	257	14.77	**43**	89.77	>1099	>12.24
14	20.89	673	32.22	**44**	90.23	>931	>10.32
15	23.08	246	10.66	**45**	108.80	145	1.33
16	25.31	107	4.23	**46**	120.90	260	2.15
19	36.60	394	10.77	**47**	126.40	91	0.72
20	38.00	156	4.11	**49**	132.00	>1055	>7.99
21	39.65	166	4.19	**50**	135.00	480	3.56
22	41.95	782	18.64	**51**	147.30	>804	>5.46
23	42.05	>844	>20.07	**52**	149.70	>1041	>6.95
24	43.22	354	8.19	**56**	160.80	>1082	>6.73
25	44.48	179	4.02	**60**	234.70	633	2.70
26	44.63	465	10.42				

[a] IC_{50}, μM. [b] LD_{50}, μM. [c] Therapeutic index, calculated as LD_{50}/IC_{50}.

function of the IC_{50}. Here, it is can be seen that **1** and **2** have very high (>1600; the open circles represent lower limits to the T.I. since no KB cell growth inhibition was seen at the highest levels tested) therapeutic index values (as defined by eq 3), which prompted us to test their effectiveness in controlling *T. gondii* proliferation in vivo. We also chose to investigate **3** (zoledronate), since it is already FDA-approved for use in humans in the context of bone resorption therapy, although as defined by eq 3, its T.I. value is much lower.

We tested all three compounds at 10 mg/kg i.p. for 10 days. For **1** at 10 mg/kg, there was an 80% protection against death, Figure 7A and for **2**, a 60% protection against death, Figure 7B. However, for **3** there was no protection against death, Figure 7C. To test whether a higher level of **1** gave enhanced protection, we increased the dosing level to 20 mg/kg, but this resulted in only a 10% survival, showing that in vivo the therapeutic index of **1** is narrow. In further experiments, we halved the

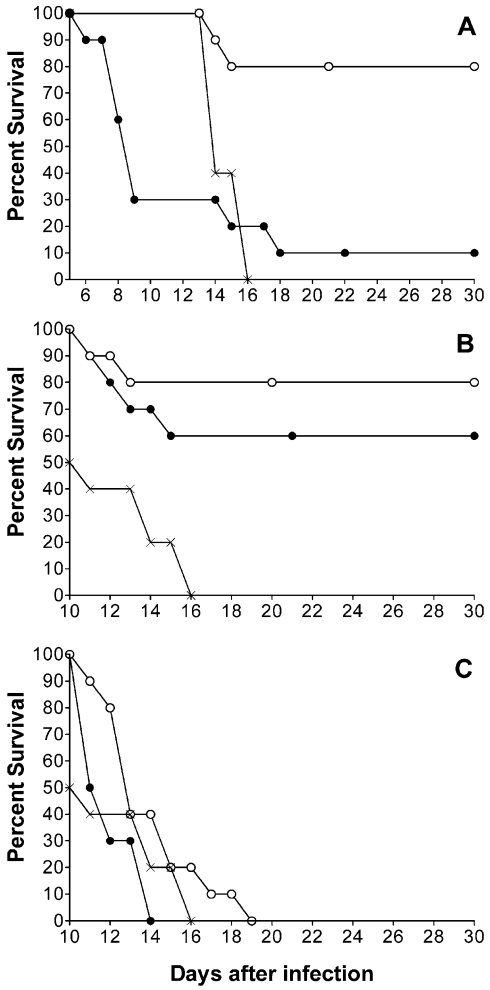

Figure 7. In vivo results for **1**−**3**. Swiss Webster mice were infected orally with five cysts of the C56 *T. gondii* strain and treatment initiated 3 days after infection via i.p. injection for 10 days. A, **1**, ○ = 10 mg/kg; ● = 20 mg/kg; x = control (PBS/DMSO). B, **2**, ○ = 5 mg/kg; ● = 10 mg/kg; x = control (PBS/DMSO). C, **3**, ○ = 5 mg/kg; ● = 10 mg/kg; x = control (PBS/DMSO). All control animals died 16 days post infection; the alkyl bisphosphonates gave up to an 80% survival rate.

dosages, for **2** and **3**. For **2**, survival increased to 80% but again with **3**, there was no protection against death, Figures 7B,C. These results, while preliminary, clearly indicate that *n*-alkyl bisphosphonates can provide up to an 80% protection against death due to *T. gondii* infection. In previous work, we found that the bisphosphonate risedronate (**6**) provided on average only about a 55% protection from death,[2] so the results reported here with the alkyl bisphosphonates represent a significant improvement, which we believe is related to the T.I. More specifically, the T.I. for risedronate (Table 4) is ~100 while for **1** and **2**, the T.I. values are ≳1600. This idea is also consistent with the observation that zoledronate (**3**), pamidronate (**20**) and alendronate (**45**) provided essentially no protection against death, consistent with their relatively low T.I. values in the *T. gondii*/KB assays (Table 4).

Conclusions

The results we have presented above are of interest for a number of reasons. First, we have obtained in vitro *T. gondii* growth inhibition results for 60, structurally diverse bisphosphonates. The two most active com-

pounds were *n*-alkyl bisphosphonates, not the more common nitrogen-containing bisphosphonates currently used in bone resorption therapy. With the alkyl bisphosphonates, activity was a function of chain length, at least for C_4-C_{10}, a pattern seen previously with *E. histolytica*, *P. falciparum* and *T. brucei*. Second, we used 3D-QSAR methods to analyze the inhibition results and found that both CoMFA and CoMSIA techniques enabled activity predictions with, on average, a factor of ~2−3 error. The CoMSIA steric and electrostatic field features correlated well with the molecular structures. Third, we tested the hypothesis that the enzyme farnesyl pyrophosphate synthase is the target for the most potent (nitrogen containing and nitrogen-free) bisphosphonates, using a *T. gondii* strain which overexpressed the FPPS enzyme. Higher levels of bisphosphonate were required in order to achieve growth inhibition with the alkyl bisphosphonates and with zoledronate, a known FPPS inhibitor, but there was no effect on atovaquone growth inhibition, which does not involve FPPS. In addition, the effects of both nitrogen containing and nitrogen-free bisphosphonates correlated with enzyme inhibition results (using human and *L. major* FPPSs). Fourth, we found that there was no effect of fosmidomycin on growth inhibition, even though *T. gondii* contains the DXR gene. Related results have been found by others with other organisms. Fifth, using a therapeutic index approach, we carried out initial testing of several bisphosphonates in vivo in a mouse model of *T. gondii* infection. Up to an 80% protection against death was obtained with the two most active alkyl bisphosphonates, an improvement over the 55% protection obtained previously with the nitrogen-containing bisphosphonates, due most likely to their lower therapeutic indices. While more work needs to be done in order to optimize side chain structure (e.g. branched side-chains, mimicking GPP), dosing regimens and bioavailability (e.g. using slow polymer release[46]), these initial results strongly support the idea that alkyl bisphosphonates may have utility in inhibiting *T. gondii* proliferation in vivo and may represent useful leads for the development of drugs against human toxoplasmosis.

Acknowledgment. This work was supported by the United States Public Health Service (NIH grant GM-65307 to E.O.), by the World Health Organization, the Illinois Governor's Venture Technology Fund and a New Investigator Award in Molecular Parasitology from Burroughs Welcome, to S.N.J.M. G.S was supported by an NIH Institutional NRSA in Molecular Biophysics NIH training grant (GM-08276). J.M.W.C. is a Jean Dreyfus Boissevain Undergraduate Scholar, funded by the Camille and Henry Dreyfus Foundation, Incorporated. We thank Ms. Linda Brown for providing excellent technical assistance.

References

(1) Martin, M. B.; Grimley, J. S.; Lewis, J. C.; Heath, H. T., 3rd; Bailey, B. N. et al. Bisphosphonates inhibit the growth of *Trypanosoma brucei*, *Trypanosoma cruzi*, *Leishmania donovani*, *Toxoplasma gondii*, and *Plasmodium falciparum*: a potential route to chemotherapy. *J. Med. Chem.* **2001**, *44*, 909−916.

(2) Yardley, V.; Khan, A. A.; Martin, M. B.; Slifer, T. R.; Araujo, F. G. et al. I*n vivo* activities of farnesyl pyrophosphate synthase inhibitors against *Leishmania donovani* and *Toxoplasma gondii*. *Antimicrob. Agents Chemother.* **2002**, *46*, 929−931.

(3) Rogers, M. J.; Watts, D. J.; Russell, R. G. Overview of bisphosphonates. *Cancer* **1997**, *80*, 1652−1660.

(4) Martin, M. B.; Sanders, J. M.; Kendrick, H.; de Luca-Fradley, K.; Lewis, J. C. et al. Activity of bisphosphonates against *Trypanosoma brucei rhodesiense*. *J. Med. Chem.* **2002**, *45*, 2904−2914.

(5) Moreno, B.; Bailey, B. N.; Luo, S.; Martin, M. B.; Kuhlenschmidt, M. et al. ^{31}P NMR of apicomplexans and the effects of risedronate on *Cryptosporidium parvum* growth. *Biochem. Biophys. Res. Commun.* **2001**, *284*, 632−637.

(6) Rodriguez, N.; Bailey, B. N.; Martin, M. B.; Oldfield, E.; Urbina, J. A. et al. Radical cure of experimental cutaneous leishmaniasis by the bisphosphonate pamidronate. *J. Infect. Dis.* **2002**, *186*, 138−140.

(7) Garzoni, L. R.; Caldera, A.; Meirelles, M. N.; de Castro, S. L.; Docampo, R. et al. Selective in vitro effects of the farnesyl pyrophosphate synthase inhibitor risedronate on *Trypanosoma cruzi*. *Int. J. Antimicrob. Agents* **2004**, *23*, 273−285.

(8) Garzoni, L. R.; Waghabi, M. C.; Baptista, M. M.; de Castro, S. L.; Meirelles, M. N. et al. Antiparasitic activity of risedronate in a murine model of acute Chagas' disease. *Int. J. Antimicrob. Agents* **2004**, *23*, 286−290.

(9) Bergstrom, J. D.; Bostedor, R. G.; Masarachia, P. J.; Reszka, A. A.; Rodan, G. Alendronate is a specific, nanomolar inhibitor of farnesyl diphosphate synthase. *Arch. Biochem. Biophys.* **2000**, *373*, 231−241.

(10) Dunford, J. E.; Thompson, K.; Coxon, F. P.; Luckman, S. P.; Hahn, F. M. et al. Structure−activity relationships for inhibition of farnesyl diphosphate synthase in vitro and inhibition of bone resorption in vivo by nitrogen-containing bisphosphonates. *J. Pharmacol. Exp. Ther.* **2001**, *296*, 235−242.

(11) Grove, J. E.; Brown, R. J.; Watts, D. J. The intracellular target for the antiresorptive aminobisphosphonate drugs in *Dictyostelium discoideum* is the enzyme farnesyl diphosphate synthase. *J. Bone Miner. Res.* **2000**, *15*, 971−981.

(12) Keller, R. K.; Fliesler, S. J. Mechanism of aminobisphosphonate action: characterization of alendronate inhibition of the isoprenoid pathway. *Biochem. Biophys. Res. Commun.* **1999**, *266*, 560−563.

(13) van Beek, E.; Pieterman, E.; Cohen, L.; Lowik, C.; Papapoulos, S. Farnesyl pyrophosphate synthase is the molecular target of nitrogen- containing bisphosphonates. *Biochem. Biophys. Res. Commun.* **1999**, *264*, 108−111.

(14) Montalvetti, A.; Bailey, B. N.; Martin, M. B.; Severin, G. W.; Oldfield, E. et al. Bisphosphonates are potent inhibitors of *Trypanosoma cruzi* farnesyl pyrophosphate synthase. *J. Biol. Chem.* **2001**, *276*, 33930−33937.

(15) Das, H.; Wang, L.; Kamath, A.; Bukowski, J. F. Vgamma2Vdelta2 T-cell receptor-mediated recognition of aminobisphosphonates. *Blood* **2001**, *98*, 1616−1618.

(16) Sanders, J. M.; Ghosh, S.; Chan, J. M.; Meints, G.; Wang, H. et al. Quantitative structure−activity relationships for $\gamma\delta$ T cell activation by bisphosphonates. *J. Med. Chem.* **2004**, *47*, 375−384.

(17) Kato, Y.; Tanaka, Y.; Miyagawa, F.; Yamashita, S.; Minato, N. Targeting of tumor cells for human gammadelta T cells by nonpeptide antigens. *J. Immunol.* **2001**, *167*, 5092−5098.

(18) Kunzmann, V.; Bauer, E.; Feurle, J.; Weissinger, F.; Tony, H. P. et al. Stimulation of gammadelta T cells by aminobisphosphonates and induction of antiplasma cell activity in multiple myeloma. *Blood* **2000**, *96*, 384−392.

(19) Wilhelm, M.; Kunzmann, V.; Eckstein, S.; Reimer, P.; Weissinger, F. et al. Gammadelta T cells for immune therapy of patients with lymphoid malignancies. *Blood* **2003**, *102*, 200−206.

(20) Wang, L.; Kamath, A.; Das, H.; Li, L.; Bukowski, J. F. Antibacterial effect of human V gamma 2V delta 2 T cells *in vivo*. *J. Clin. Invest.* **2001**, *108*, 1349−1357.

(21) Eberl, M.; Hintz, M.; Reichenberg, A.; Kollas, A. K.; Wiesner, J. et al. Microbial isoprenoid biosynthesis and human gammadelta T cell activation. *FEBS Lett.* **2003**, *544*, 4−10.

(22) Jomaa, H.; Wiesner, J.; Sanderbrand, S.; Altincicek, B.; Weidemeyer, C. et al. Inhibitors of the nonmevalonate pathway of isoprenoid biosynthesis as antimalarial drugs. *Science* **1999**, *285*, 1573−1576.

(23) Testa, C. A.; Brown, M. J. The methylerythritol phosphate pathway and its significance as a novel drug target. *Curr. Pharm. Biotechnol.* **2003**, *4*, 248−259.

(24) Szabo, C. M.; Matsumura, Y.; Fukura, S.; Martin, M. B.; Sanders, J. M. et al. Inhibition of geranylgeranyl diphosphate synthase by bisphosphonates and diphosphates: a potential route to new bone antiresorption and antiparasitic agents. *J. Med. Chem.* **2002**, *45*, 2185−2196.

(25) Sanders, J. M.; Gomez, A. O.; Mao, J.; Meints, G. A.; Van Brussel, E. M. et al. 3-D QSAR investigations of the inhibition of *Leishmania major* farnesyl pyrophosphate synthase by bisphosphonates. *J. Med. Chem.* **2003**, *46*, 5171−5183.

(26) Ghosh, S.; Chan, J. M.; Lea, C. R.; Meints, G. A.; Lewis, J. C. et al. Effects of bisphosphonates on the growth of *Entamoeba histolytica* and *Plasmodium* species *in vitro* and *in vivo*. *J. Med. Chem.* **2004**, *47*, 175−187.

(27) Dobrowolski, J. M.; Sibley, L. D. Toxoplasma invasion of mammalian cells is powered by the actin cytoskeleton of the parasite. *Cell* **1996**, *84*, 933−939.
(28) *Sigma Plot 5.0*; SPSS Inc.: Chicago.
(29) Soldati, D.; Boothroyd, J. C. Transient transfection and expression in the obligate intracellular parasite *Toxoplasma gondii*. *Science* **1993**, *260*, 349−352.
(30) Araujo, F. G.; Khan, A. A.; Slifer, T. L.; Bryskier, A.; Remington, J. S. The ketolide antibiotics HMR 3647 and HMR 3004 are active against *Toxoplasma gondii* in vitro and in murine models of infection. *Antimicrob. Agents Chemother.* **1997**, *41*, 2137−2140.
(31) *SYBYL 6.9*; Tripos Inc.: St. Louis.
(32) Clark, M.; Cramer, R. D., 3rd; Van Opdenbosch, N. Validation of the General Purpose Tripos 5.2 Force Field. *J. Comput. Chem.* **1989**, *10*, 982−1012.
(33) Powell, M. J. D. Restart procedures for the conjugate gradient method. *Math. Programming* **1977**, *12*, 241−254.
(34) Press, W. H. *Numerical recipes in C: the art of scientific computing*; Cambridge University Press: New York, 1988; p 324.
(35) Gasteiger, J.; Marsili, M. Iterative partial equalization of orbital electronegativity: a rapid access to atomic charges. *Tetrahedron* **1980**, *36*, 3219−3328.
(36) Kotsikorou, E.; Oldfield, E. A quantitative structure−activity relationship and pharmacophore modeling investigation of aryl-X and heterocyclic bisphosphonates as bone resorption agents. *J. Med. Chem.* **2003**, *46*, 2932−2944.
(37) Tarshis, L. C.; Proteau, P. J.; Kellogg, B. A.; Sacchettini, J. C.; Poulter, C. D. Regulation of product chain length by isoprenyl diphosphate synthases. *Proc. Natl. Acad. Sci.* **1996**, *93*, 15018−15023.
(38) Bush, B. L.; Nachbar, R. B., Jr. Sample-distance partial least squares: PLS optimized for many variables, with application to CoMFA. *J. Comput. Aided Mol. Des.* **1993**, *7*, 587−619.
(39) Cramer, R. D., 3rd; Patterson, D. E.; Bunce, J. D. Recent advances in comparative molecular field analysis (CoMFA). *Prog. Clin. Biol. Res.* **1989**, *291*, 161−165.
(40) Klebe, G.; Abraham, U.; Mietzner, T. Molecular similarity indices in a comparative analysis (CoMSIA) of drug molecules to correlate and predict their biological activity. *J. Med. Chem.* **1994**, *37*, 4130−4146.
(41) Montalvetti, A.; Fernandez, A.; Sanders, J. M.; Ghosh, S.; Van Brussel, E. et al. Farnesyl pyrophosphate synthase is an essential enzyme in Trypanosoma brucei. *In vitro* RNA interference and *in vivo* inhibition studies. *J. Biol. Chem.* **2003**, *278*, 17075−17083.
(42) McFadden, D. C.; Tomavo, S.; Berry, E. A.; Boothroyd, J. C. Characterization of cytochrome b from *Toxoplasma gondii* and Q(o) domain mutations as a mechanism of atovaquone-resistance. *Mol. Biochem. Parasitol.* **2000**, *108*, 1−12.
(43) Hosfield, D. J.; Zhang, Y.; Dougan, D. R.; Broun, A.; Tari, L. W. et al. Structural basis for bisphosphonate-mediated inhibition of isoprenoid biosynthesis. *J. Biol. Chem.* **2004**, *279*, 8526−8529.
(44) Altincicek, B.; Hintz, M.; Sanderbrand, S.; Wiesner, J.; Beck, E. et al. Tools for discovery of inhibitors of the 1-deoxy-D-xylulose 5-phosphate (DXP) synthase and DXP reductoisomerase: an approach with enzymes from the pathogenic bacterium *Pseudomonas aeruginosa*. *FEMS Microbiol. Lett.* **2000**, *190*, 329−333.
(45) Neu, H. C.; Kamimura, T. In vitro and in vivo antibacterial activity of FR-31564, a phosphonic acid antimicrobial agent. *Antimicrob. Agents Chemother.* **1981**, *19*, 1013−1023.
(46) Khanna, S. C.; Green, J. Methanediphosphonic acid formulations with ion exchangers. U.S. Patent *5,344,825*, 1994.

JM040132T